

Structure of ${}^7\text{Be}$ and ${}^{63}\text{Cu}$ determined from the ${}^{63}\text{Cu}({}^6\text{Li}, {}^7\text{Be}){}^{62}\text{Ni}$ reaction*

G. M. Hudson, K. W. Kemper, G. E. Moore, and M. E. Williams
Department of Physics, The Florida State University, Tallahassee, Florida 32306

(Received 2 April 1975)

Angular distributions have been measured for the reaction ${}^{63}\text{Cu}({}^6\text{Li}, {}^7\text{Be}_{0,1}){}^{62}\text{Ni}_{0,1}$ at $E({}^6\text{Li}) = 34$ MeV in the angular range $2-52.5^\circ$ (lab). Exact finite-range distorted-wave-Born-approximation (DWBA) calculations were not able to reproduce the shape of the angular distributions even though similar calculations with the same optical model parameters were able to describe the ${}^{62}\text{Ni}({}^7\text{Li}, {}^6\text{He}){}^{63}\text{Cu}$ reaction. Elastic scattering data for ${}^7\text{Li} + {}^{62}\text{Ni}$ and ${}^6\text{Li} + {}^{63}\text{Cu}$ were reanalyzed with the optical model assuming a real radius given by $R = 1.2 A_T^{1/3}$ instead of the previously used $R = 1.2(A_T^{1/3} + A_P^{1/3})$. The optical model fits to the elastic scattering data and the finite-range DWBA calculations for the ${}^{62}\text{Ni}({}^7\text{Li}, {}^6\text{He})$ reaction data were equivalent with both optical parameter sets while the ${}^{63}\text{Cu}({}^6\text{Li}, {}^7\text{Be})$ fit was greatly improved. The shape of the forward angle ${}^{63}\text{Cu}({}^6\text{Li}, {}^7\text{Be}_{0,1}){}^{62}\text{Ni}_0$ data indicates that ${}^7\text{Be}_1$ has a larger $1p_{3/2}/1p_{1/2}$ ratio than found in the ground state of ${}^7\text{Be}$. Ratios of $1p_{3/2}/1p_{1/2}$ strengths in ${}^7\text{Be}_{0,1}$ extracted by fitting the shape of the forward angle data with finite-range DWBA calculations of the cross sections are in excellent agreement with the calculations of Cohen and Kurath. In addition, the spectroscopic factor for ${}^{63}\text{Cu}$ is in good agreement with values found from other reactions when the Cohen and Kurath results for ${}^7\text{Be}$ are assumed. The spectroscopic factor for the component in the ${}^{63}\text{Cu}$ ground state wave function which corresponds to ${}^{62}\text{Ni}(2^+) \otimes 2p_{3/2}$ has also been extracted. An upper limit for the magnitude of the cross section for the reaction ${}^{63}\text{Cu}({}^6\text{Li}, {}^9\text{Be})$ has been determined.

NUCLEAR REACTIONS ${}^{63}\text{Cu}({}^6\text{Li}, {}^7\text{Be})$ measured $\sigma(\theta)$ at $E({}^6\text{Li}) = 34$ MeV for $\theta = 2-52.5^\circ$, $\Delta\theta = 2.5^\circ$. Deduced $S({}^{62}\text{Ni}_{0,1})$ and $S({}^7\text{Be}_{0,1})$ from finite-range DWBA analysis. ${}^{63}\text{Cu}({}^6\text{Li}, {}^9\text{Be})$ measured σ at 15, 20, and 25° .

I. INTRODUCTION

Heavy-ion induced direct single particle transfer reactions have not been extensively used to extract nuclear spectroscopic information because the complexity of the structure of the projectile and ejectile makes the analysis of the data more difficult than in the equivalent light-ion case. Also, the simplifying assumptions of the zero-range distorted-wave-Born-approximation (DWBA) cannot be made. However, the added complications present in heavy-ion induced transfer reactions can often provide new information such as the spin of the final state populated in the reaction.¹⁻³ In a study of the ${}^{62}\text{Ni}({}^7\text{Li}, {}^6\text{He}){}^{63}\text{Cu}$ reaction^{3,4} it was shown that $2p_{3/2}$ single particle states could be easily distinguished from $2p_{1/2}$ single particle states. Also, the shapes of the measured angular distributions were well described by finite-range DWBA calculations and the extracted spectroscopic factors were in good agreement with light-ion measurements. These results imply a considerable understanding of the $({}^7\text{Li}, {}^6\text{He})$ reaction. Recent measurements⁵ of the ${}^{40}\text{Ca}({}^{13}\text{C}, {}^{12}\text{C}){}^{41}\text{Ca}$ and ${}^{40}\text{Ca}({}^{13}\text{C}, {}^{14}\text{N}){}^{39}\text{K}$ reactions have shown that the $({}^{13}\text{C}, {}^{12}\text{C})$ reaction could be described by finite-range DWBA calculations while the $({}^{13}\text{C}, {}^{14}\text{N})$ reaction could not. These re-

sults indicated the need for further studies of Li induced single particle transfer reactions. The present work reports on measurements of the ${}^{63}\text{Cu}({}^6\text{Li}, {}^7\text{Be}){}^{62}\text{Ni}$ reaction. The experimental data consist of angular distributions for the reaction populating the ground and first excited states of ${}^{62}\text{Ni}$ with ${}^7\text{Be}$ in its ground and first excited states. The results have been analyzed in terms of the exact finite-range DWBA which yielded spectroscopic factors for ${}^7\text{Be}$ and ${}^{63}\text{Cu}$ as well as $1p_{3/2}$ to $1p_{1/2}$ relative strengths for the first two states of ${}^7\text{Be}$.

II. EXPERIMENTAL PROCEDURES

Both a Heinicke direct radial extraction negative ion source⁶ and sputter source⁷ were used to produce ${}^6\text{Li}^-$ for injection into the Florida State University super FN tandem Van de Graaff accelerator. Average beam currents on target varied between 100 and 300 nA at 34 MeV.

Free standing ${}^{63}\text{Cu}$ (enriched to 99.8%) targets 80 to 100 $\mu\text{g}/\text{cm}^2$ thick were made by conventional evaporation techniques. Thicker targets (~ 300 $\mu\text{g}/\text{cm}^2$) were evaporated onto carbon backings for use at large angles.

Two separate scattering systems were used in the experiment, a large general purpose scattering

chamber⁸ and a quadrupole spectrometer.⁹ The reaction data for the laboratory angular range 15 to 52.5° in 2.5° steps were taken in the scattering chamber with an angular acceptance of 0.30°. The 2 to 15° data were taken with the quadrupole spectrometer in 1 and 2.5° steps with an angular acceptance of 0.5°. The band pass and solid angle of the quadrupole spectrometer were defined by normalizing the 15° quadrupole data to the 15° data taken in the scattering chamber.

The reaction products were detected by ΔE - E silicon surface barrier counter telescopes. The signals were amplified, digitized, and then transferred and stored in E , ΔE pairs via a Camac interface in an EMR-6130 computer. The E , ΔE pairs were then displayed on a storage scope and gates were drawn around the particle types of interest with a light pen. These gates were then used to sort the events into linear energy spectra.

A monitor counter was used to determine target stability and to normalize the data over the measured angular range. A typical spectrum taken in the scattering chamber is shown in Fig. 1. The energy resolution was 150–175 keV FWHM (full width at half-maximum). The yields for the reaction groups were extracted by a Gaussian peak fitting program.¹⁰ The product of target thickness times the detector solid angle, which is necessary to determine the reaction absolute cross section, was found by measuring ${}^6\text{Li} + {}^{63}\text{Cu}$ elastic scattering at 32 and 34 MeV at the angles 15, 20, and 25° (lab) and comparing these results to the cross sections determined by White and Kemper⁴ at 32 MeV. The absolute error in the $({}^6\text{Li}, {}^7\text{Be})$ reaction occurring from a combination of charge integration and statistical errors in the normalization data and the absolute error

reported in Ref. 4 is 12%. The relative errors in the $({}^6\text{Li}, {}^7\text{Be})$ reaction measurements ranged between 9 and 22%, coming from a combination of statistical and peak fitting errors.

In addition to the ${}^7\text{Be}$ data, attempts were made to observe the ${}^{63}\text{Cu}({}^6\text{Li}, {}^9\text{Be}){}^{60}\text{Ni}$ reaction at 15, 20, and 25° (lab). However, only an upper limit for the cross section of 5 $\mu\text{b}/\text{sr}$ at 25° could be made. These observations are in agreement with the predicted three particle spectroscopic factors calculated by Kurath and Millener¹¹ for the ${}^9\text{Be} \rightarrow {}^6\text{Li} + (1p)^3$ system. Also observed was the $({}^6\text{Li}, {}^7\text{Li})$ reaction which was several times more prolific than the $({}^6\text{Li}, {}^7\text{Be})$ reaction. The high density of states in ${}^{62}\text{Cu}$ and poor energy resolution due to the thick targets used made the simultaneous study of the $({}^6\text{Li}, {}^7\text{Li})$ and $({}^6\text{Li}, {}^7\text{Be})$ reactions unfeasible.

III. EXPERIMENTAL RESULTS

The ${}^{63}\text{Cu}({}^6\text{Li}, {}^7\text{Be}){}^{62}\text{Ni}$ spectrum in Fig. 1 shows that the two strongest states excited in ${}^{62}\text{Ni}$ are the 0^+ ground state and the 1.17 MeV 2^+ first excited state. These two states will be labeled ${}^{62}\text{Ni}_0$ and ${}^{62}\text{Ni}_1$. For each of the ${}^{62}\text{Ni}$ state excited, two peaks occur corresponding to ${}^7\text{Be}$ in its $\frac{3}{2}^-$ ground and $\frac{1}{2}^-$ 0.43 MeV first excited states. These two states will be labeled ${}^7\text{Be}_0$ and ${}^7\text{Be}_1$. The angular distributions for these four states are shown in Fig. 2 where it can be seen that the shapes of the angular distributions are all similar for angles greater than 20°. The ratio of cross sections for ${}^7\text{Be}_0/{}^7\text{Be}_1$ for ${}^{62}\text{Ni}$ in its ground state averaged over the angular range 20 to 35° was 1.77 in good agreement with Groeneveld *et al.*,¹² who found this ratio to be 1.60 for the reaction ${}^{14}\text{N}({}^6\text{Li}, {}^7\text{Be}){}^{13}\text{C}$ at $E({}^6\text{Li}) = 32$ MeV.

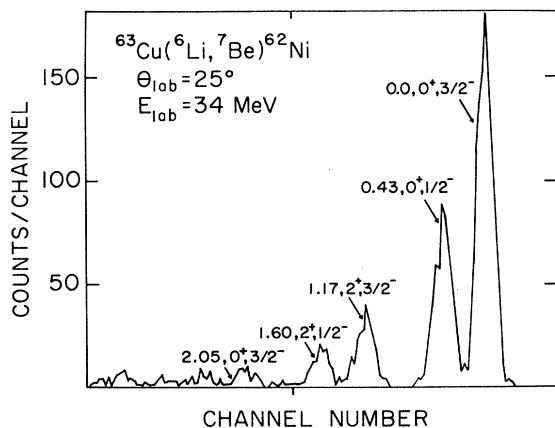


FIG. 1. Sample spectrum for the ${}^{63}\text{Cu}({}^6\text{Li}, {}^7\text{Be}){}^{62}\text{Ni}$ reaction. The peaks are labeled by the combined energy and J^π of the states excited in ${}^{62}\text{Ni}$ and ${}^7\text{Be}$.

IV. ANALYSIS

A. DWBA analysis

The optical model parameters reported in Ref. 4 were used in exact finite-range DWBA calculations performed with the code MERCURY¹³ for the reactions ${}^{63}\text{Cu}({}^6\text{Li}, {}^7\text{Be}_{0,1}){}^{62}\text{Ni}_0$. It was assumed in these calculations that the optical model parameters which describe ${}^7\text{Li} + {}^{62}\text{Ni}$ elastic scattering also describe ${}^7\text{Be} + {}^{62}\text{Ni}$. The ${}^7\text{Li} + {}^{62}\text{Ni}$ elastic scattering measurements⁴ were done at 34 MeV, while in the present study the ${}^7\text{Be}$ energy is about 32 MeV and the ${}^6\text{Li} + {}^{63}\text{Cu}$ measurements⁴ were done at the energies 28.1, 30.1, and 32.1 MeV; in the present study the ${}^6\text{Li}$ energy is 34 MeV. However, the lack of any observable energy

dependence of the ${}^6\text{Li}$ optical model parameters over the 4 MeV range studied in Ref. 4 indicates that the parameters obtained earlier should be applicable in the present study. The standard form⁴ of the optical model potential has been assumed in the present work. The structure of ${}^{63}\text{Cu}$ was assumed to be composed of a $2p_{3/2}$ proton coupled to the ground state of ${}^{62}\text{Ni}$, and the structure of both states in ${}^7\text{Be}$ was assumed to be a combination of $1p_{3/2}$ and $1p_{1/2}$ proton states coupled to ${}^6\text{Li}$ in its ground state. The Cohen and Kurath¹⁴ values for the $1p_{3/2}$ and $1p_{1/2}$ components in ${}^7\text{Be}$ were assumed. The bound state geometrical parameters used were $r_0 = 1.25$ fm and $a = 0.65$ fm; a spin-orbit factor $\lambda = 25$ was also used in the calculations. The bound proton potential depths were determined by varying the potential depths until the proper proton binding energies were found. The experimental cross section is related to the

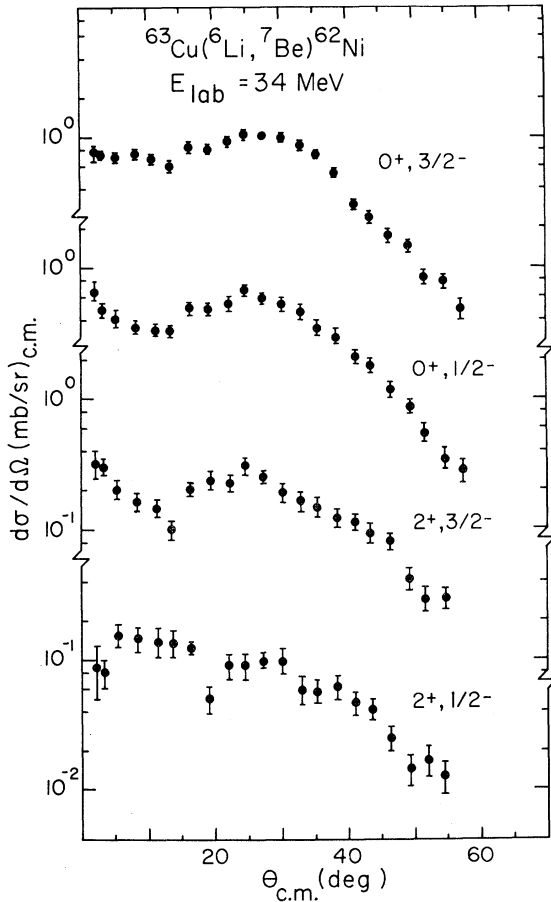


FIG. 2. Angular distributions of the ${}^{63}\text{Cu}({}^6\text{Li}, {}^7\text{Be}){}^{62}\text{Ni}$ reaction. The angular distributions are labeled by the J^π of the states excited in ${}^{62}\text{Ni}$ and ${}^7\text{Be}$.

calculated cross section by

$$\frac{d\sigma}{d\Omega}(\theta)_{\text{exp}} = C^2 S({}^{62}\text{Ni}) \left[C^2 S({}^7\text{Be})_{p_{3/2}} \frac{d\sigma}{d\Omega}(\theta)_{\text{MERC}} + C^2 S({}^7\text{Be})_{p_{1/2}} \frac{d\sigma}{d\Omega}(\theta)_{\text{MERC}} \right], \quad (1)$$

where S is the appropriate spectroscopic factor and C is the appropriate isospin Clebsch-Gordan coefficient. The calculations normalized to the data and the data are shown in Fig. 3. The calculations give a reasonable description of the data for angles greater than 15° but the rise at extreme forward angles is much greater than observed in the data. Several changes were made in the calculations to try to improve the fit at forward angles. These changes included increasing the bound state radius parameter in the ${}^6\text{Li}+p$ system from 1.25 to 1.50 fm and using equivalent imaginary surface absorptive optical model potentials instead of volume imaginary potentials in the finite-range DWBA calculations. No improvement in the fit to the data was obtained from either change. The amounts of the $1p_{3/2}$ and $1p_{1/2}$ components in ${}^7\text{Be}$ were allowed to be free parameters in the calculations and the relative weights of the two components were found by fitting the data. It was still not possible to fit both the grazing angle region ($20\text{--}35^\circ$) and the forward angle region simultaneously. Analyses of ${}^7\text{Li}$ induced single nucleon transfer reactions in the

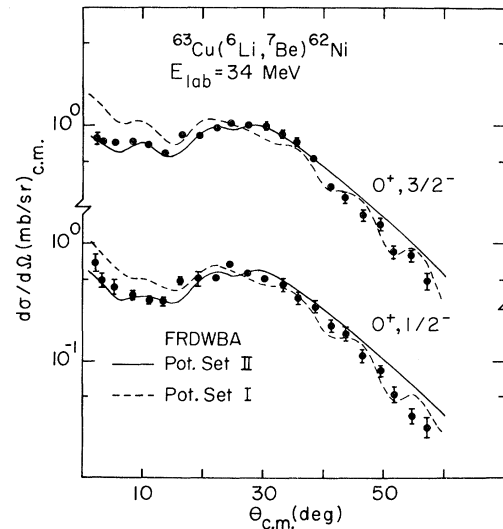


FIG. 3. Angular distributions for transitions to the ${}^{62}\text{Ni}$ ground state with ${}^7\text{Be}$ in its ground and first excited states. The curves are finite-range DWBA calculations with the two optical potential parameter sets given in Table I.

TABLE I. Optical model parameters.

	Set	U (MeV)	r_R^a (fm)	a_R (fm)	W (MeV)	r_I^a (fm)	a_I (fm)	r_c (fm)
${}^6\text{Li} + {}^{62}\text{Ni}$	I	47.4	1.78	0.58	11.6	1.70	0.90	1.78
	II	176.6	1.21	0.81	22.4	1.70	0.80	1.78
${}^7\text{Li} + {}^{63}\text{Cu}$	I	49.7	1.78	0.58	8.5	1.78	1.01	1.78
	II	199.0	1.22	0.86	21.6	1.78	0.70	1.78

$$^a R = rA_T^{1/3}.$$

$1p^{15}$ and $2s-1d^{16}$ shells have used optical model parameters with a smaller real radius of interaction than that used by White and Kemper.⁴ These finite-range DWBA calculations have had considerable success in describing the transfer data. The elastic scattering data of Ref. 4 were analyzed with the interaction radii defined by $R = r_0 A_T^{1/3}$ instead of $R = r_0 (A_T^{1/3} + A_P^{1/3})$. A real radius parameter r_0 of 1.2 fm was used. The search procedure followed with the program JIB¹⁷ varied the real potential (U) and the imaginary potential (W) with the real radius parameter r_0 fixed at 1.2 fm until the best fit to the data was found. Then the real diffuseness a_r and the imaginary radius r_i were varied followed by the real radius r_0 and the imaginary diffuseness a_i . The best fit set of potential parameters is Set II in Table I.

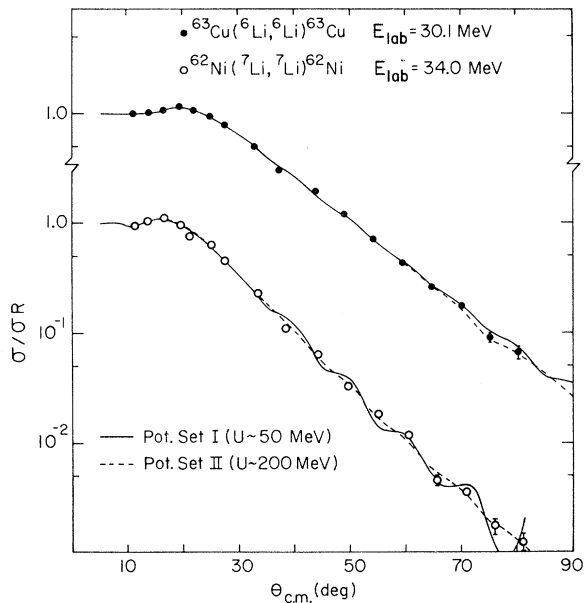


FIG. 4. Angular distributions for the elastic scattering of ${}^6\text{Li} + {}^{63}\text{Cu}$ at 30.1 MeV and ${}^7\text{Li} + {}^{62}\text{Ni}$ at 34 MeV taken from Ref. 4. The curves are the results of optical model calculations carried out with the parameter sets given in Table I.

The fit to the data is shown in Fig. 4. Both sets of optical model parameters reproduce the elastic scattering cross sections equally well.

The ${}^{63}\text{Cu}({}^6\text{Li}, {}^7\text{Be}, {}_0, 1)$ cross sections recalculated with the new set of optical model parameters are shown in Fig. 3. The forward angle fit is considerably improved with this set of optical model parameters. The ${}^{62}\text{Ni}({}^7\text{Li}, {}^6\text{He})$ reaction to the first two states in ${}^{63}\text{Cu}$ was also recalculated and the results of these calculations and the data from Ref. 4 are shown in Fig. 5. The magnitude of the two calculated cross sections relative to each other are as shown in Fig. 5. Again, the fit to the data is as good as obtained with the shallower potential set. As can be seen in Figs. 3, 4, and 5, the major difference in the cross sections calculated with the two sets of optical parameters is that the Set I angular distributions are more structured than the Set II angular distributions. This difference arises from the stronger absorption of Set II than Set I. Normally, in the angular regions where the calculated structure in the angular distributions is greatest the cross sections are small, making the presence of the structure difficult to confirm experimentally. However, the sensitivity of the $({}^6\text{Li}, {}^7\text{Be})$ reaction at forward angles to the optical parameters permitted a clear choice between the two parameter sets.

B. Spectroscopic factors

The cross section for the ${}^{63}\text{Cu}({}^6\text{Li}, {}^7\text{Be}){}^{62}\text{Ni}$ reaction depends on both the structure of ${}^7\text{Be}$ and ${}^{63}\text{Cu}$, as can be seen from Eq. (1). The allowed angular momentum transfers L for this reaction are given by the selection rules

$$|l_1 - l_2| \leq L \leq l_1 + l_2$$

and

$$|J_1 - J_2| \leq L \leq J_1 + J_2,$$

where l_1 (l_2) and J_1 (J_2) are the orbital and total angular momenta of the transferred proton in the target and the ejectile. Since ${}^{63}\text{Cu}$ can be written as ${}^{62}\text{Ni} \otimes 2p_{3/2}$ and ${}^7\text{Be}$ as ${}^6\text{Li}$ with both $1p_{3/2}$ and

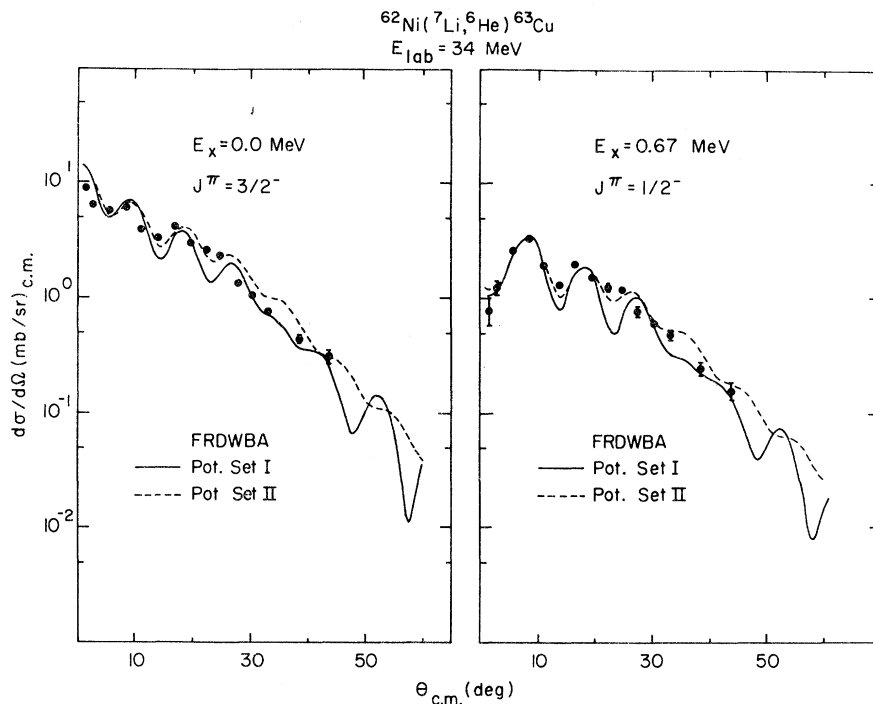


FIG. 5. Angular distributions for the $^{62}\text{Ni}(^7\text{Li}, ^6\text{He})^{63}\text{Cu}$ reaction to the ground and first excited states of ^{63}Cu taken from Ref. 4. The curves are the results of finite-range DWBA calculations with the optical parameter sets in Table I.

$1p_{1/2}$ components, then the $1p_{3/2}$ component of ^7Be permits $L=0, 1$, and 2 , while the $1p_{1/2}$ component allows $L=1$ and 2 . The difference between the two components should be observable at small

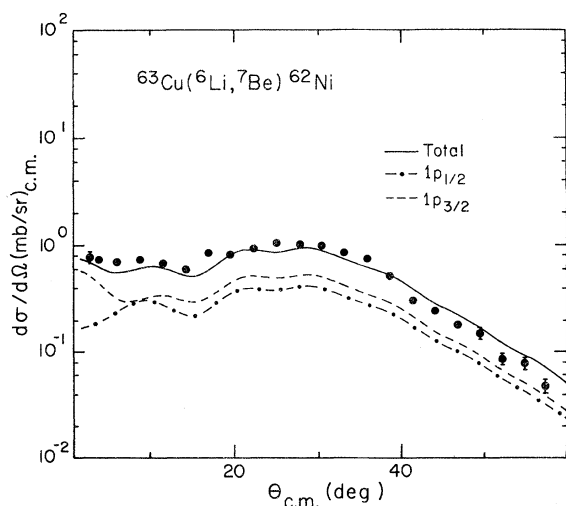


FIG. 6. Angular distribution for the $^{63}\text{Cu}(^6\text{Li}, ^7\text{Be})^{62}\text{Ni}$ reaction showing the contribution to the total cross section from the $1p_{3/2}$ and $1p_{1/2}$ components in ^7Be .

angles, where the $L=0$ contribution has a maximum. It has been shown earlier³ with the $^{62}\text{Ni}(^7\text{Li}, ^6\text{He})^{63}\text{Cu}$ reaction that $2p_{3/2}$ states can be distinguished from $2p_{1/2}$ states by the presence of the $L=0$ component in the transfer. In Fig. 2, it can be seen that at small angles the cross section for $^7\text{Be}_1$ rises more than for $^7\text{Be}_0$ implying a larger $1p_{3/2}$ component in $^7\text{Be}_1$ than in $^7\text{Be}_0$ as predicted by Cohen and Kurath.¹⁴ In Fig. 6 the forward angle portion of the $(^6\text{Li}, ^7\text{Be})$ data is shown with finite-range DWBA calculations for the $1p_{3/2}$ and $1p_{1/2}$ components in ^7Be . The finite-range DWBA calculations show that differences in the cross section components occur only for angles less than 10° .

The product of absolute spectroscopic factors $C^2S(^{62}\text{Ni})C^2S(^7\text{Be})$ appearing in Eq. (1) can be extracted by fitting the finite-range DWBA calculations for the $^7\text{Be}_0$ and $^7\text{Be}_1$ transitions to the data in the region of the classical grazing angle; the product is 0.57 for the $^{62}\text{Ni}_0$ - $^7\text{Be}_0$ transition and 0.77 for the $^{62}\text{Ni}_0$ - $^7\text{Be}_1$ transition. The ratio of total $1p$ strength in $^7\text{Be}_1$ to $^7\text{Be}_0$ is then 1.35 in good agreement with the Cohen and Kurath¹⁴ value of 1.24. This ratio was found to be 1.55 with the $^6\text{Li}(^3\text{He}, d)^7\text{Be}$ reaction¹⁸ in reasonable agreement with the present work. The spectroscopic factor

TABLE II. Spectroscopic factor products.

$C^2S({}^{62}\text{Ni}_0)C^2S({}^7\text{Be}_0) = 0.57$
$C^2S({}^{62}\text{Ni}_0)C^2S({}^7\text{Be}_1) = 0.77$
$C^2S({}^{62}\text{Ni}_1)C^2S({}^7\text{Be}_0) = 0.16$
$C^2S({}^{62}\text{Ni}_1)C^2S({}^7\text{Be}_1) = 0.20$

products are summarized in Table II.

To extract absolute spectroscopic factors for either ${}^7\text{Be}$ or ${}^{62}\text{Ni}$, assumptions must be made about the knowledge of one or the other of the two. From other reaction studies, the range of values for $C^2S({}^{62}\text{Ni})$ reported is from 0.56 to 0.78. If it is assumed $C^2S({}^7\text{Be}_0)$ is 1.0, then $C^2S({}^{62}\text{Ni})$ is 0.57.

TABLE III. Spectroscopic factors.

	Cohen and Kurath		Exp.		${}^{62}\text{Ni}_0$	${}^{62}\text{Ni}_1$
	$p_{3/2}$	$p_{1/2}$	$p_{3/2}$	$p_{1/2}$	Exp.	Exp.
${}^7\text{Be}_0$	0.43	0.29	0.37	0.35	0.79	0.22
${}^7\text{Be}_1$	0.85	0.04	0.95	0.00	0.81	0.21

If the Cohen and Kurath value for $C^2S({}^7\text{Be}_0)$ is assumed, the $C^2S({}^{62}\text{Ni})$ would be 0.79. Both values fall in the range of previously obtained values. The absolute spectroscopic factor results are summarized in Table III where it was assumed that the total $1p$ strength for the ground state of ${}^7\text{Be}$ was equal to the Cohen and Kurath value, and the other numbers given then reflect this assumption. These values assume no renormalization factors are needed in the DWBA calculation.

The ratio of $1p_{3/2}/1p_{1/2}$ strength in the two states of ${}^7\text{Be}$ excited can be extracted by fitting the two components in the calculated cross section to the experimental data for the extreme forward angle region (2.2–16.5° c.m.). The values labeled exp in Table III were obtained in this manner, and the best fits to the data are shown in Fig. 7. The values obtained agree extremely well with the ratios calculated by Cohen and Kurath¹⁴ and show roughly equal contributions of $1p_{3/2}$ and $1p_{1/2}$ in the ${}^7\text{Be}$ ground state and that the first excited state of ${}^7\text{Be}$ is almost totally of $1p_{3/2}$ character. Since the shape of the calculations depends on the assumptions made, these extracted ratios should be treated with some caution until other targets have been examined so that the importance of multistep contributions can be better evaluated.

The cross section for the transition to the 2^+ state in ${}^{62}\text{Ni}$ was also calculated assuming a component in the ground state of ${}^{63}\text{Cu}$ corresponding to ${}^{62}\text{Ni}(2^+) \otimes 2p_{3/2}$. The calculations and the data are shown in Fig. 7 and the extracted spectroscopic factors are given in Table III. The spectroscopic factors are in good agreement with results (~0.20) obtained from an analysis of α -particle scattering on ${}^{63}\text{Cu}$ ¹⁹ and both works indicate a sizable ${}^{62}\text{Ni}(2^+)$ component in ${}^{63}\text{Cu}$. Since there are many other components that can also contribute to the reaction, for example ${}^{62}\text{Ni} \otimes 1f_{5/2}$, it is not possible to perform a complete calculation for this transition until more complete structure calculations for ${}^{63}\text{Cu}$ are performed. In addition, full multistep calculations need to be carried out since two-step transitions were seen to be important in the ${}^{62}\text{Ni}({}^7\text{Li}, {}^6\text{He})$ reaction.⁴ The poor fit to the data at the forward angles clearly indicates that effects other than direct one-step pickup contributions are present.

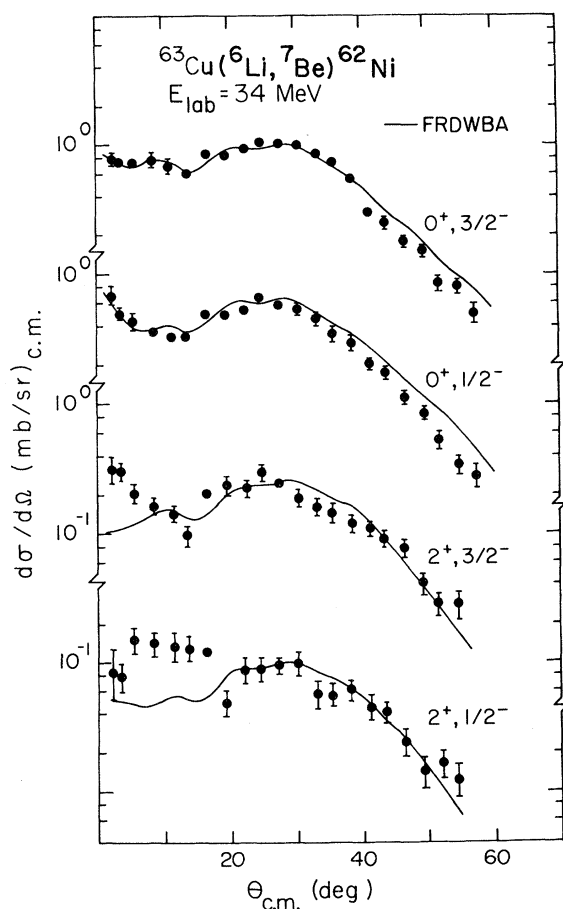


FIG. 7. Angular distributions and finite-range DWBA calculations for the ${}^{63}\text{Cu}({}^6\text{Li}, {}^7\text{Be}_0, {}^7\text{Be}_1){}^{62}\text{Ni}_{0,1}$ reactions. The curves for the transitions to the ground state of ${}^{62}\text{Ni}$ were obtained by varying the ratio of $1p_{3/2}$ to $1p_{1/2}$ in ${}^7\text{Be}$ until the best fit to the data was obtained. For the transitions to the first excited state of ${}^{62}\text{Ni}$ only the pickup of a $2p_{3/2}$ proton was assumed.

V. CONCLUSIONS

In the present work it has been shown that the shape of the forward angle portion of the angular distribution for the $^{63}\text{Cu}(^6\text{Li}, ^7\text{Be})$ reaction calculated with exact finite-range DWBA is very dependent on the optical model parameters used. To fit the proton pickup reaction data, a real potential with a smaller radius of interaction $R = 1.2A_T^{1/3}$ rather than $R = 1.2(A_T^{1/3} + A_P^{1/3})$ which is normally used in heavy-ion optical model parameters was necessary. The type of optical model parameters which described the ($^6\text{Li}, ^7\text{Be}$) data have also been shown to describe Li induced single particle transfer data on $1p$ and $2s-1d$ shell nuclei. The present work indicates that ^7Li optical parameters are a reasonable substitute for measured ^7Be parameters. The extracted spectro-

scopic factors for $^{63}\text{Cu} - ^{62}\text{Ni} + p$ are at the upper end of the range of values obtained for other reactions if the Cohen and Kurath results for $^6\text{Li} + p \rightarrow ^7\text{Be}$ are assumed. More importantly, the extracted $1p_{3/2}/1p_{1/2}$ ratios for the ground and first excited states of ^7Be have been found to be in excellent agreement with the Cohen and Kurath calculations. The magnitude of the cross section to the $^{62}\text{Ni} 2^+$ first excited state indicates the presence of a sizable contribution to the ^{63}Cu ground state from an excited ^{62}Ni core.

The authors wish to thank R. Puigh, G. Norton, C. Delaune, G. D. Gunn, and R. L. White for their assistance in taking the data and to thank L. A. Charlton and D. Robson for many helpful discussions and for furnishing the finite range DWBA code MERCURY.

*Work supported in part by the National Science Foundation Grants Nos. NSF-MPS-7503767, NSF-GU-2612, and NSF-GJ-367.

¹D. G. Kovar, F. D. Becchetti, B. G. Harvey, F. Pühlhofer, J. Mahoney, D. W. Miller, and M. S. Zisman, *Phys. Rev. Lett.* **29**, 1023 (1972).

²M. J. Schneider, C. Chasman, E. H. Auerbach, A. J. Baltz, and S. Kahana, *Phys. Rev. Lett.* **31**, 321 (1973); C. Chasman, S. Kahana, and M. J. Schneider, *ibid.* **31**, 1074 (1973).

³R. L. White, K. W. Kemper, L. A. Charlton, and G. D. Gunn, *Phys. Rev. Lett.* **32**, 892 (1974).

⁴R. L. White and K. W. Kemper, *Phys. Rev. C* **10**, 1372 (1974).

⁵P. D. Bond, J. D. Garrett, O. Hansen, S. Kahana, M. J. LeVine, and A. Z. Schwarzschild, in *Proceedings of the International Conference on Reactions between Complex Nuclei, Nashville, Tennessee, 10-14 June, 1974*, edited by R. L. Robinson, F. K. McGowan, J. B. Ball, and J. H. Hamilton (North-Holland, Amsterdam, 1974), Vol. I, p. 55.

⁶E. Heinicke and H. Baumann, *Nucl. Instrum. Methods* **58**, 125 (1968).

⁷R. Middleton and C. T. Adams, *Nucl. Instrum. Methods* **118**, 329 (1974).

⁸G. D. Gunn, T. A. Schmick, L. Wright, and J. D. Fox,

Nucl. Instrum. Methods **113**, 1 (1974).

⁹G. R. Morgan, G. D. Gunn, M. B. Greenfield, N. R. Fletcher, J. D. Fox, D. McShan, and L. Wright, *Nucl. Instrum. Methods* **123**, 439 (1975).

¹⁰H. A. Kauffman and G. D. Gunn, program PHENIX (unpublished).

¹¹D. Kurath and D. J. Millener, *Nucl. Phys.* **A238**, 269 (1975).

¹²K. O. Groeneveld, A. Richter, U. Strohmusch, and B. Zeidman, *Phys. Rev. Lett.* **27**, 1806 (1971).

¹³L. A. Charlton, *Phys. Rev. C* **8**, 146 (1973); L. A. Charlton and D. Robson, Florida State University Technical Report No. 5. MERCURY (unpublished).

¹⁴S. Cohen and D. Kurath, *Nucl. Phys.* **A101**, 1 (1967).

¹⁵P. Schumacher, N. Ueta, H. H. Duhm, K. I. Kubo, and W. J. Klages, *Nucl. Phys.* **A212**, 573 (1973).

¹⁶G. E. Moore, K. W. Kemper, and L. A. Charlton, *Phys. Rev. C* **11**, 1099 (1975).

¹⁷F. G. Perey, *Phys. Rev.* **131**, 745 (1963); A. W. Obst, Florida State University Technical Report JIB (unpublished).

¹⁸H. Lüdecke, T. Wan-Tjin, H. Werner, and J. Timmer, *Nucl. Phys.* **A109**, 676 (1968).

¹⁹M. Bosman, P. Leleux, P. C. Macq, J. P. Meulders, and C. Pirart, *Phys. Rev. C* **11**, 628 (1975).